Green Chemistry

PAPER

View Article Online
View Journal | View Issue

Cite this: *Green Chem.*, 2026, **28**, 5482

H-bond mediated photocatalyzed oxidation of oximes under visible light and air. A general route toward dioxazoles, oxadiazoles and isoxazoles

Younes Massad, [a] Arkadiusz Zych, [a] Mathieu Duttine, [b] Dario M. Bassani, [a] Frédéric Robert [a] and Yannick Landais *[a]

The development of sustainable and efficient synthetic methods for nitrogen-containing heterocycles remains a central focus in modern organic chemistry. Oxazoles and their derivatives are of significant interest in both academic and industrial research owing to their broad spectrum of biological activities and frequent occurrence in natural products. Here we present a photocatalyzed visible-light-induced oxidation of oximes as a versatile strategy for the construction of three distinct heterocyclic skeletons, *i.e.* dioxazoles, oxadiazoles and isoxazoles. This photochemical process features a broad substrate scope, functional group tolerance, and high regioselectivity delivering products in yields of up to 92%. By leveraging a metal-free photocatalyst (4-DPAIPN) and visible light irradiation at 456 nm under atmospheric air conditions, the method enables selective oxidative cyclization of structurally diverse oxime precursors. Mechanistic investigations using EPR, fluorescence quenching experiments and transient absorption spectroscopy suggest the formation of an iminoxyl radical as a key intermediate, generated through the oxidation of the oxime bound to the photocatalyst through hydrogen bonding. This interaction is proposed to contribute to the selective oxidation of the oxime by the oxidized photocatalyst. Subsequent oxidation of the iminoxyl radical into a nitrile oxide, followed by [3 + 2] cycloaddition with ketones, nitriles, or alkynes, affords streamlined access to the corresponding heterocycles. Overall, this photocatalytic strategy provides a green alternative to conventional methods, minimizing wastes, while delivering valuable nitrogen–oxygen atoms containing heterocycles with potential applications in pharmaceutical and materials chemistry.

Received 17th December 2025,
Accepted 25th February 2026

DOI: 10.1039/d5gc06840a

rsc.li/greenchem

Green foundation

1. The oxidation of oximes under conventional protocols typically relies on stoichiometric oxidants, resulting in substantial waste generation. The present work employs an organophotocatalyst and visible light as a renewable energy source to promote this transformation using air as the sole oxidant in an environmentally benign solvent. This strategy thus achieves high atom economy, minimizes waste production, and enhances overall efficiency.
2. This work replaces the traditional two-step synthesis of nitrogen–oxygen–containing heterocycles, which typically relies on stoichiometric, often toxic and costly oxidants, with a one-pot, operationally simple, and sustainable oxidation of oximes. The transformation is driven by visible-light irradiation using an environmentally benign photocatalyst and air as the sole oxidant, providing access to a wide range of valuable heterocycles in generally high yields
3. This work contributes to the development of oxidation protocols that employ air as the sole oxidant under environmentally benign activation modes, including low-energy visible light. Moreover, the weak interactions between the photocatalyst and substrates that facilitate the oxidation process described herein highlight opportunities for further catalyst design and broader application in green chemistry.

Introduction

Five-membered heterocycles are ubiquitous in nature and occupy a central position in pharmaceutical, agrochemical, and materials research. Among these, oxadiazoles,[1] isoxazoles,[2] and dioxazoles[3] have recently garnered considerable attention owing to their distinctive chemical and biological properties (Fig. 1). These heterocycles are characterized by high thermal stability, aromaticity (for **I** and **II**), and the potential for extensive structural modification. Oxadiazoles are particularly notable for their wide-ranging applications in medicinal chemistry, functioning as antimicrobial, anticancer, anti-inflammatory, and central nervous system (CNS)-active agents (*e.g.*, ibotenic acid).[4] They also serve as the core scaffold in therapeutics such as ataluren, used in the treatment of cystic

[a]*Univ. Bordeaux, CNRS, Bordeaux INP, ISM, UMR 5255, F-33400 Talence, France. E-mail: yannick.landais@u-bordeaux.fr*
[b]*Univ. Bordeaux, CNRS, Bordeaux INP, ICMCB, UMR 5026, F-33600 Pessac, France*

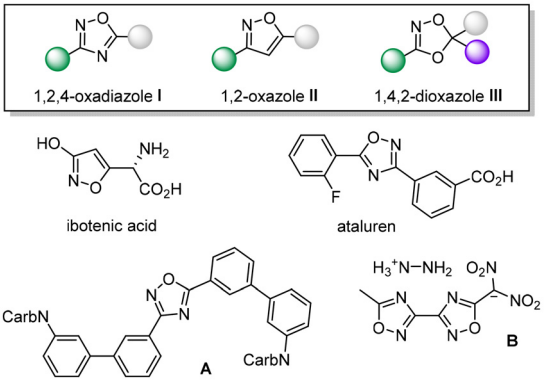

Fig. 1 Generic structures of oxadiazoles, oxazoles and dioxazoles. Some examples of natural and synthetic members of these families of heterocycles (CarbN: carbazole).

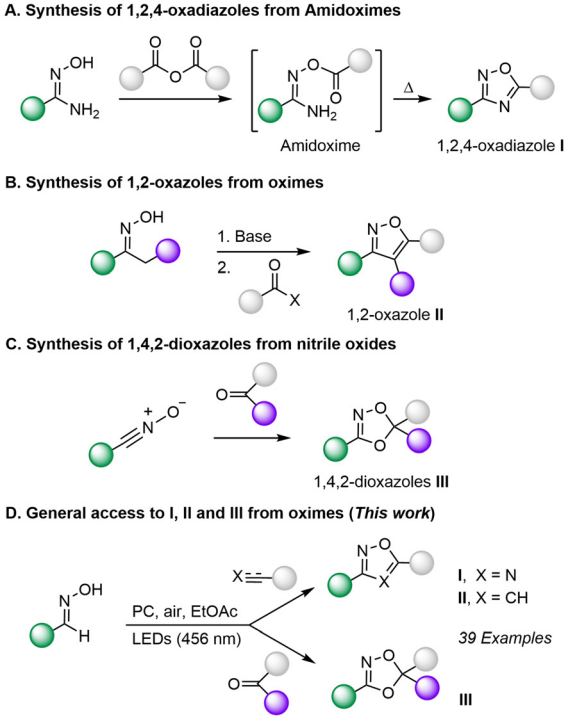

Fig. 2 (A) synthesis of oxadiazoles from amidoximes. (B) Synthesis of isoxazoles from oximes. (C) Synthesis of dioxazoles from nitrile oxides. (D) Synthesis of 1,2,4-oxadiazole **I**, 1,2-isoxazole **II** and 1,4,2-dioxazole **III** from oximes (this work).

fibrosis (Fig. 1).[5] Moreover, oxadiazoles are well established as bioisosteres of esters and amides, enhancing metabolic stability and bioavailability in drug design. Isoxazoles likewise represent privileged motifs in numerous bioactive molecules, including antibiotics and antitumor agents, due to their robustness and bioisosteric behavior. Although less extensively studied, dioxazoles **III** have emerged as promising entities in both medicinal and coordination chemistry. Beyond their biological relevance, these heterocycles play significant roles in agrochemistry as structural components of herbicides, fungicides, and insecticides. In the field of materials science, they contribute to the development of high-performance organic electronic materials such as organic light-emitting diodes (OLEDs; *e.g.*, **A**),[6] organic solar cells, and semiconductors, owing to their electron-transporting and photophysical properties. More recently, oxadiazole and dioxazole derivatives have also been investigated as energetic materials (*e.g.*, **B**).[7] The structural versatility and multifunctional character of these heterocycles thus continue to drive innovation across diverse areas of chemistry and applied science.

Several methodologies have been reported for the synthesis of these heterocycles and were recently reviewed.[8] These include cyclodehydration of acyclic precursors, rearrangement, and condensation processes (Fig. 2A and B), such as the classical reaction between amidoximes and carboxylic acid derivatives commonly employed for the preparation of 1,2,4-oxadiazoles.[8,9] Among these strategies, the [3 + 2] cycloaddition represents the most general and versatile approach for accessing all three heterocyclic frameworks.[10] This transformation involves the reaction of 1,3-dipoles (*e.g.*, nitrile oxides or nitrones) with suitable dipolarophiles (such as alkynes, alkenes, nitriles, or carbonyl compounds), thereby providing a unified, modular, convergent, and regioselective route to the desired heterocycles. Moreover, this methodology allows broad structural diversity and exhibits excellent functional-group tolerance, rendering it the most general synthetic route among the currently available methods. Nitrile oxides (Fig. 2C), which constitute the most effective precursors for the target heterocycles, are typically generated by oxidation of the corresponding oximes *via* the formation of intermediate chloroximes, which are subsequently converted into nitrile oxides under basic conditions.[11] Conventional oxidation protocols for the conversion of oximes into nitrile oxides generally rely on stoichiometric oxidants,[11,12] including *N*-chlorosuccinimide, *t*-BuOCl, *m*-CPBA, $ArI(OAc)_2$, DMDO, NaClO, chloramine-T, $PhICl_2$, MnO_2, CrO_3, or, more recently, NaCl/oxone. While these methods are effective, they invariably produce substantial amounts of waste.

To overcome this environmental limitation, molecular oxygen appeared as an attractive alternative oxidant—clean, abundant, and sustainable—for the generation of nitrile oxides. The oxidation of oximes was envisioned to proceed through reactive oxygen species (ROS) derived from molecular oxygen, either by photoinduced electron transfer (PET) leading to superoxide radical anion $O_2^{\bullet-}$, or by energy transfer (EnT) resulting in singlet oxygen $^1O_2$.[13] Both pathways could ultimately afford the nitrile oxide *via* a dehydrogenation process, minimizing waste and aligning with the principles of green chemistry, with H_2O_2 as the sole by-product.

Despite its conceptual appeal, this strategy has received very limited attention to date,[14] in contrast to recent advances in oxime oxidation that have predominantly focused on electrochemical methods.[15] Herein, we report the development of an efficient and general photocatalytic oxidation of oximes employing molecular oxygen as the terminal oxidant and a

readily available organophotocatalyst (PC). This transformation enables the regioselective synthesis of 1,2,4-oxadiazoles (**I**), oxazoles (**II**), and 1,4,2-dioxazoles (**III**) through the direct oxidation of oximes in the presence of nitriles, alkynes, and ketones, respectively (Fig. 2D). A plausible mechanistic scenario is advanced on the basis of reactive-intermediate trapping, fluorescence-quenching studies, and Electron Paramagnetic Resonance (EPR) spectroscopy, which collectively indicate the formation of a key iminoxyl radical and the presence of $^1O_2$ and superoxide as reactive oxygen species. Notably, complementary transient absorption spectroscopy and ^{1}H NMR experiments also suggest hydrogen-bonding interactions between the photocatalyst and the oxime substrate, thereby facilitating oxidation of the latter. This uncommon hydrogen-bond-driven photocatalysis is appealing and appears to be more general, potentially enabling broader applications.

Results and discussion

A. Photocatalyzed oxidation of oximes in the presence of ketones, nitriles and alkynes

Several photosensitizers—including Rose Bengal, methylene blue, porphyrins, and zinc phthalocyanines—are known to efficiently sensitize molecular oxygen under light irradiation, generating various reactive oxygen species (ROS).[13,16] These sensitizers were therefore evaluated in a model oxidation between 4-fluorobenzaldoxime **1a** and an excess of 3,3,3-trifluoroacetophenone **2a** under an atmosphere of air. However, none of these conditions afforded the desired 1,4,2-dioxazole **3a** (see SI for details). More promising results were obtained with 4-CzIPN as the photocatalyst in CH_3CN under irradiation at 456 nm (entry 1, Table 1).[17] Notably, employing the same sensitizer in DCE or *t*-BuOH resulted in significantly diminished yields or complete suppression of reactivity, underscoring the crucial role of the solvent (entries 2 and 3). A marked improvement was observed in EtOAc, which was ultimately identified as the optimal solvent for this transformation (entry 4). Control experiments confirmed the essential role of each reaction component: no product formation was observed in the absence of the photocatalyst (entry 5), light (entry 6), or oxygen (entry 7), with **1a** being largely recovered unchanged. These findings demonstrate that the process is indeed photosensitized and oxygen-dependent. Variation of the irradiation wavelength only marginally affected the reaction outcome (entry 8). Encouraged by the initial success with 4-CzIPN, we next examined additional members of this photocatalyst family.[18] 4-DAPTPN showed poor activity (entry 9 and SI), whereas 4-*t*-BuCzIPN afforded improved yields, albeit with the formation of several by-products (entry 10). The best results were obtained with 4-DPAIPN,[19] which delivered **3a** in 57% yield as determined by NMR analysis (entry 11). A key improvement was achieved by increasing the reaction concentration from 0.036 M to 0.1 M, affording an isolated yield of 81% after 8 h of irradiation (entry 12). Further increasing the concentration (entry 13) did not lead to additional enhancement in yield.

Table 1 Optimization of the reaction conditions between oxime **1a** and ketone **2a**

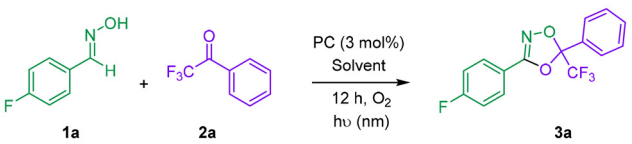

1a + **2a** → **3a**

Entry[a]	PC	λ (nm)	Solvent	Yield[b] (%)
1	4-CzIPN	456	CH_3CN	22
2	4-CzIPN	456	*t*-BuOH	0
3	4-CzIPN	456	DCE	8
4	4-CzIPN	456	EtOAc	(31)
5[c]	—	456	EtOAc	0
6[c]	4-CzIPN	—	EtOAc	0
7[d]	4-CzIPN	456	EtOAc	2
8	4-CzIPN	467	EtOAc	14
9	4-DPATPN	456	EtOAc	Traces
10	4-*t*-ButCzIPN	456	EtOAc	35
11	4-DPAIPN	456	EtOAc	57
12[e]	**4-DPAIPN**	**456**	**EtOAc (0.1 M)**	**(81)**
13[f]	4-DPAIPN	456	EtOAc (0.2 M)	(69)

[a] Typical reaction conditions was set up as follows: **1a** (1 mmol) and **2a** (3 mmol), photocatalyst (3 mol%) in solution in the given solvent was irradiated using Kessil lamps (456 nm) for 8–12 hours at 35 °C under air. [b] Yields were calculated by ^{19}F NMR using 1,4-bis-(trifluoromethyl) benzene as an internal standard. Isolated yield under brackets. [c] Starting oxime recovered. [d] Reaction was done under an N_2 atmosphere, the reaction led only to by-products (aldehyde and acid). [e] Monitoring of the reaction indicates consumption of starting material after 8 h. [f] Monitoring of the reaction indicates consumption of starting material after 3 h.

With the optimized conditions in hand, the scope and limitations of the transformation were next investigated (Scheme 1). The reaction proceeded efficiently with a broad range of aryloximes **1a–q** bearing either electron-donating or electron-withdrawing substituents, irrespective of their position on the aromatic ring, affording the corresponding 1,4,2-dioxazoles **3a–q** in yields of up to 92%. Notably, the conversion of **1c** to **3c** was complete within 2 h, underscoring the enhanced reactivity of substrates containing electron-deficient substituents. Most reactions were conducted on a millimolar scale, demonstrating the practicality of the protocol. Scale-up to 10 mmol was demonstrated by the preparation of **3g** in 72% yield. In this case, distillation of the reaction mixture prior to work-up enabled ~84% solvent recovery (SI). Aliphatic oximes also proved to be competent substrates, furnishing the desired products **3o–q** under the standard conditions. In contrast, oximes derived from heteroaromatic systems such as pyridine and furan failed to deliver **3m–n**, likely due to the susceptibility of these electron-rich heteroarenes to oxidative degradation by ROS. Variation of the carbonyl component was also possible, as evidenced by the successful synthesis of **3l**; however, only activated ketones were found to afford the corresponding adducts (SI).

The methodology was then extended to the photocatalytic oxidation of oximes in the presence of nitriles as dipolaro-

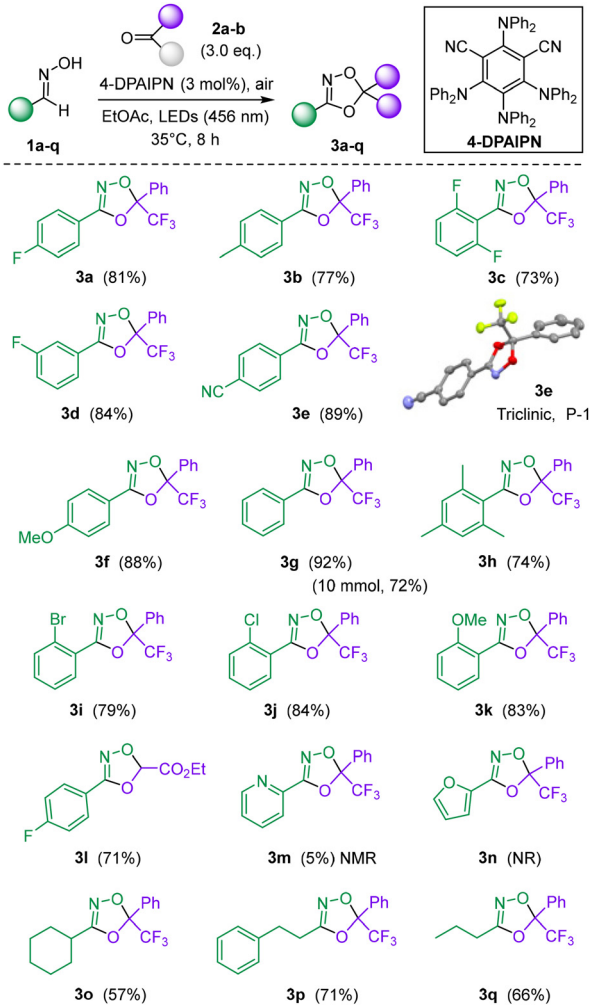

Scheme 1 Synthesis of 1,4,2-dioxazoles **3a–q** through photocatalyzed oxidation of oxime **1a–q** in the presence of ketones **2a–b**.

philes, enabling access to the corresponding 1,2,4-oxadiazole derivatives **5** (Scheme 2). This transformation represents a prominent route to 1,2,4-oxadiazoles and has therefore attracted considerable synthetic interest.[8a] The reaction proceeded smoothly with both unsubstituted and aryl nitriles bearing electron-withdrawing substituents, affording products **5a–f** in good to excellent yields. Interestingly, for compound **5f**, further reaction of the remaining nitrile moiety with an additional equivalent of oxime was unsuccessful, suggesting that formation of the electron-rich oxadiazole ring significantly diminishes the reactivity of the residual nitrile group. In contrast, aliphatic nitriles (*e.g.*, **5h**) and electron-rich nitriles (*e.g.*, **5i)** exhibited low or negligible reactivity, in line with previous reports indicating that Lewis acid activation (*e.g.*, $BF_3{\cdot}OEt_2$)[20] is typically required to promote this transformation. Attempts to achieve the reaction in the presence of $BF_3{\cdot}OEt_2$ under the current photocatalytic conditions, however, proved unsuccessful.

The methodology was subsequently extended to the oxidation of oximes in the presence of alkynes to afford the

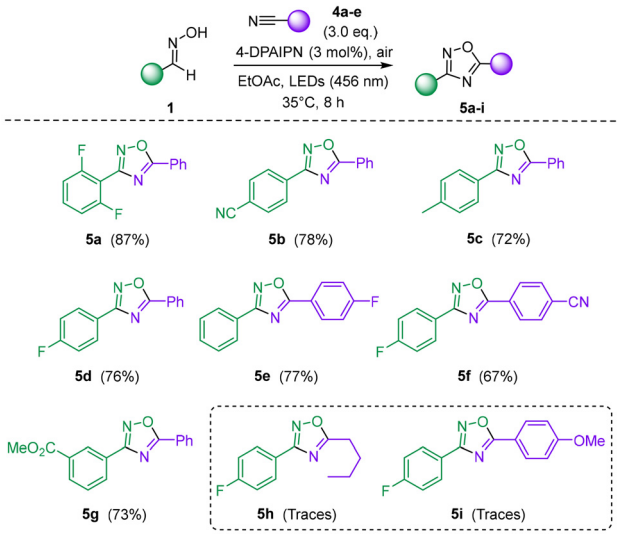

Scheme 2 Synthesis of 1,2,4-oxadiazoles **5a–i** through photocatalyzed oxidation of oximes **1** in the presence of nitriles **4a–e**.

corresponding isoxazoles **7** (Scheme 3). Cycloadditions involving preformed nitrile oxides, chloroximes, or nitroalkanes with alkynes constitute some of the most established approaches for the synthesis of isoxazoles.[8b] Under the previously optimized conditions (Table 1), a diverse set of oximes was successfully oxidized in the presence of both aryl- and alkyl-substituted alkynes, providing the desired isoxazoles in

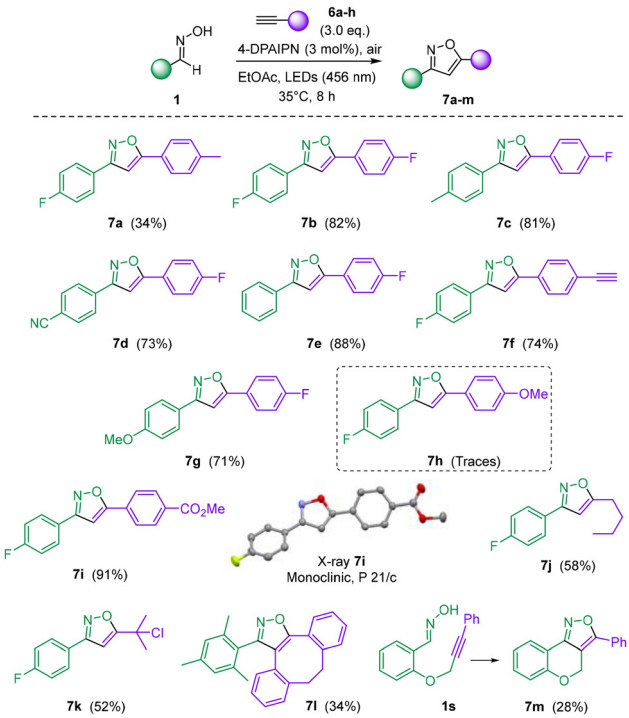

Scheme 3 Synthesis of isoxazoles **7a–m** through photocatalyzed oxidation of oximes **1** in the presence of alkynes **6a–h**.

generally high yields (Scheme 3). Attempts were made to recycle the excess alkyne during the preparation of **7a** and **7i**, leading to a recovery of the corresponding alkyne up to 1.92 eq. and 1.34 eq., respectively (SI). Consistent with observations made for aryl nitriles, alkynylarenes bearing electron-withdrawing substituents afforded higher yields than their electron-rich counterparts (*e.g.*, **7b–e** *vs.* **7h**). The structure of **7i** was unambiguously confirmed by single-crystal X-ray diffraction, thereby establishing the regioselectivity of the cycloaddition as depicted. In contrast to the nitrile series, terminal alkynes bearing alkyl substituents proved to be competent dipolarophiles, furnishing the corresponding isoxazoles **7j–k** with the indicated regioselectivity. Interestingly, bis-alkyne **6c** yielded exclusively the mono-addition product **7f**, even in the presence of an excess of oxime **1a**, likely due to electronic deactivation following the initial cycloaddition event. Attempts to employ an aliphatic oxime in combination with an aryl alkyne failed to deliver the corresponding heterocycle. The extension of the reaction to strained cycloalkynes was also examined using 4-dibenzocyclooctynol (DIBO, **6h**), a substrate well known for its exceptionally high reactivity toward nitrile oxides and its application in orthogonal bioconjugation chemistry.[21] When directly mixed with mesityl oxime **1h**, DIBO underwent rapid decomposition under the standard reaction conditions. However, the slow addition of a solution of DIBO in EtOAc to **1h** *via* syringe pump enabled the formation of isoxazole **7l**, albeit in moderate yield. Finally, an intramolecular variant employing alkynyloxime **1s** successfully furnished the tricyclic isoxazole **7m** in modest yield.

B. Mechanistic studies

A series of experiments was undertaken to gain mechanistic insight into the photocatalytic transformation of oximes into heterocycles **I–III**. The reaction between **1a** and **2a** was first performed in the presence of 1 eq. of TEMPO, which resulted in a substantial decrease in yield (18% *vs.* 81%; see SI), thereby supporting the involvement of a radical pathway. To examine the participation of superoxide radical anion and/or singlet oxygen ($^1O_2$), probe **9**, which is known to differentiate between electron-transfer (Type I) and singlet oxygen (Type II) processes, was subjected to irradiation in the presence of 4-DPAIPN under an oxygen atmosphere. Formation of trace amounts of adducts **10a–b** was observed, indicating the generation of both $^1O_2$ and $O_2^{\bullet-}$ species (Fig. 3A).[16b] Further evidence was obtained using boronic acid **11**, a recently developed probe capable of distinguishing between singlet oxygen and superoxide.[22] Upon irradiation, **11** selectively yielded phenol **12** without detectable fluoride anion in the ^{19}F NMR spectrum, thereby confirming the formation of superoxide during the photooxygenation mediated by 4-DPAIPN. ROS quenching experiments using NaN_3, DABCO, and *p*-benzoquinone (Fig. 3B) further corroborated the concurrent involvement of both $^1O_2$ and $O_2^{\bullet-}$ in the reaction medium.[23] Interestingly, 1,3-diphenylisobenzofuran (DPBF) neither produced the expected dione nor inhibited the formation of **3a** under the reaction conditions.

To identify possible intermediates arising from the oxidation of oximes, additional experiments were conducted (Fig. 3C). When α,β-unsaturated oxime **13** was subjected to the standard conditions, the reaction furnished predominantly the corresponding aldehyde **14c**, along with trace amounts of nitrile **14b** and imine **14d** (detected by GC–MS; see SI). More notably, heterocycle **14a** was detected, strongly suggesting the involvement of an iminoxyl radical intermediate.[24] Reid *et al.*, recently postulated the participation of iminoyl or oximidoyl radicals generated *via* C–H abstraction during the electro-

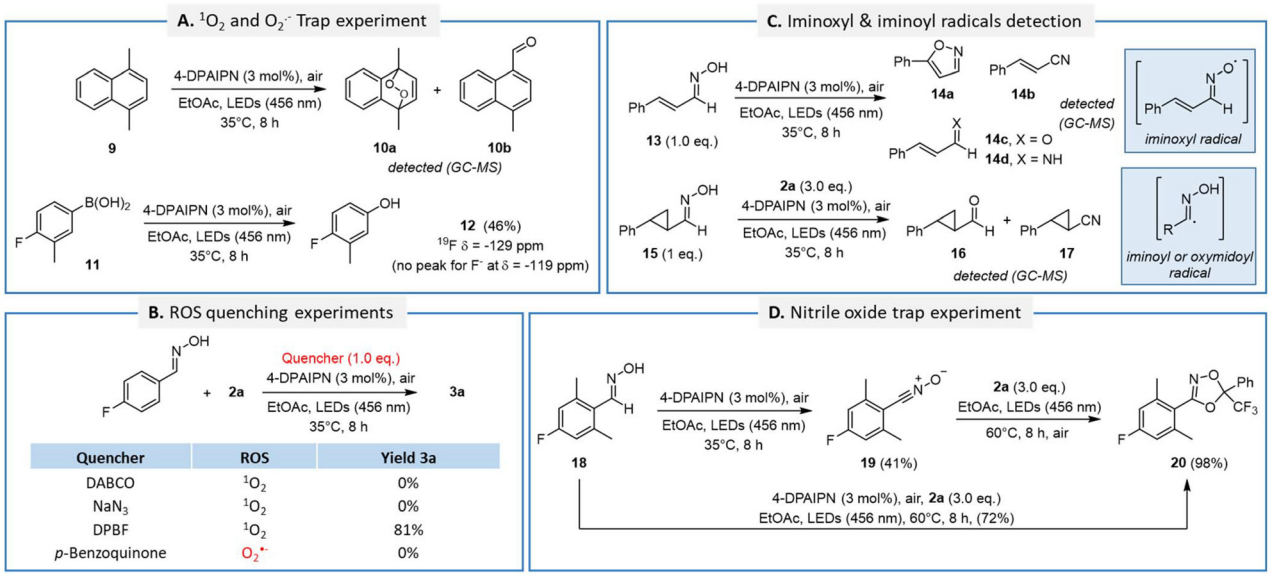

Fig. 3 (A) $^1O_2$ and $O_2^{\bullet-}$ trapping experiments. (B) ROS-quenching experiments. (C) Experiments to detect potent iminoxyl and iminoyl radicals. (D) Nitrile-oxide trapping experiments.

chemical oxidation of oximes.[15b] To examine whether a similar radical species might be involved under our photochemical conditions, oxime **15** was subjected to the standard reaction conditions. Only trace amounts of aldehyde **16** and nitrile **17** were detected by GC–MS, with no evidence of cycloaddition products or cyclopropane ring opening. These results effectively rule out the participation of an iminoyl radical intermediate (Fig. 3C). Finally, the potential formation of a nitrile oxide intermediate through oxidation of the iminoxyl radical was evaluated using oxime **18**. When the latter was subjected to the optimized conditions in the absence of a dipolarophile, the corresponding stable nitrile oxide **19** was isolated in 41% yield (Fig. 3D). Compound **19** was subsequently shown to undergo cycloaddition with **2a** under the same conditions to afford the corresponding adduct **20** in high yield. Moreover, when **18** was reacted under the standard conditions in the presence of **2a**, the desired cycloadduct **3h** was obtained in excellent yield, providing strong evidence that nitrile oxides act as key intermediates in the photocatalytic process.

Fluorescence quenching experiments were next performed to identify the species capable of interacting with the excited state of the photocatalyst. As shown in Fig. 4A and B, molecular oxygen—but not oxime **1a**—efficiently quenched the fluorescence of the excited photocatalyst 4-DPAIPN*. Like the well-studied chromophore 4-CzIPN, 4-DPAIPN exhibits thermally activated delayed fluorescence (TADF) behavior, characterized by the reversible interconversion between its first excited singlet (S_1) and triplet (T_1) states.[18] The absence of any measurable decrease in emission intensity upon addition of **1a** indicates that neither of these excited states is quenched by the substrate. In contrast, the Stern–Volmer analysis of quenching by O_2 displayed pronounced downward curvature, which we attribute to the presence of two interconverting excited states that are both quenched by O_2 (Fig. 4B). This observation contrasts with the findings of Ishitani and coworkers, who reported that only the T_1 state of 4-DPAIPN is susceptible to quenching by molecular oxygen.[25] To investigate this discrepancy, the excited-state lifetime (τ_s) of the S_1 state was determined from the prompt component of the emission decay using time-correlated single-photon counting (see SI). Comparing τ_s in EtOAc solutions purged with argon, air, or O_2 evidenced a variation (τ_s = 2.7, 2.1, and 1.7 ns, respectively). The value obtained under argon is similar to that previously reported in *N*,*N*-dimethylacetamide (2.9 ns), and we may thus assign the decrease in τ_s to quenching by O_2. From these data, the bimolecular quenching rate constant was estimated to be 2.1×10^{10} M^{-1} s^{-1}, a value close to that expected for diffusion-controlled quenching in EtOAc (2.4×10^{10} M^{-1} s^{-1}).[26]

Electron Paramagnetic Resonance (EPR) experiments were subsequently conducted under the optimized reaction conditions in the presence of 5,5-dimethyl-1-pyrroline *N*-oxide (DMPO) as a radical trapping agent. The spectrum recorded shortly after irradiation (Fig. 4C) was characteristic of the superoxide radical anion ($O_2^{\bullet-}$).[27] In aprotic organic solvents

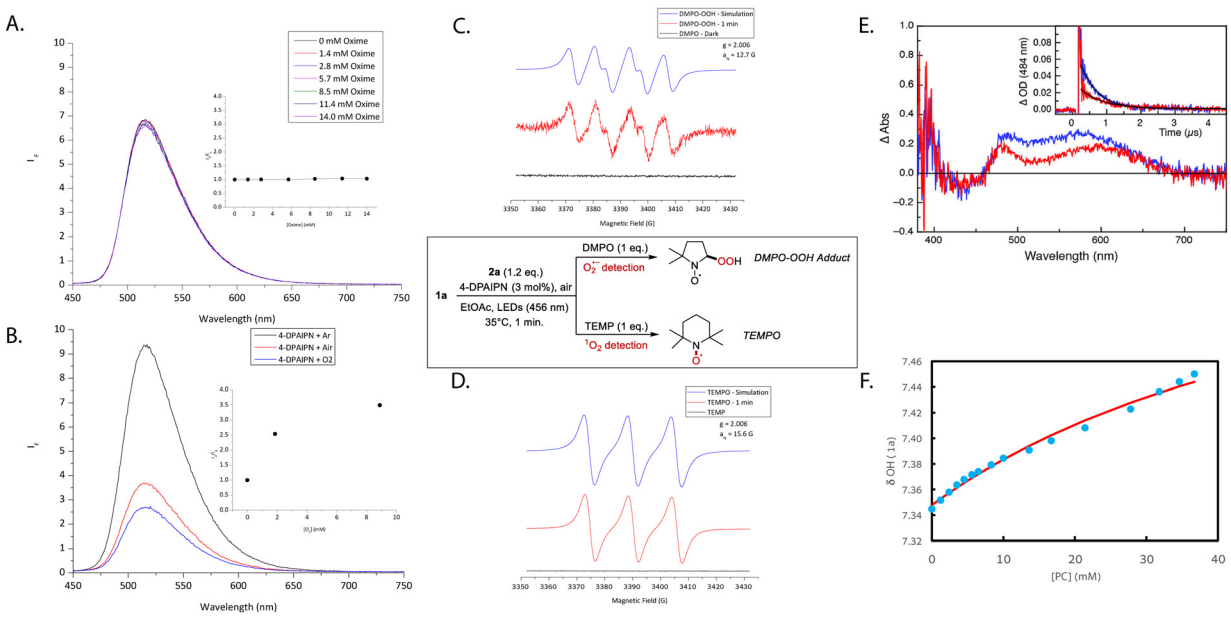

Fig. 4 (A) Fluorescence quenching experiments of 4-DPAIPN (1×10^{-5} M) using various concentration of oxime **1a** in EtOAc. (B) Fluorescence quenching experiments of 4-DPAIPN (1×10^{-5} M) using various concentration of O_2 in EtOAc. (C) EPR spectrum of a 0.1 M solution of DMPO in EtOAc (1 equiv.) with oxime **1a** (1 equiv.) and ketone **2a** (1 equiv.), 4-DPAIPN (0.5 mol%). (D) EPR spectrum of a 0.1 M solution of TEMP in EtOAc (1 equiv.) with oxime **1a** (1 equiv.) and ketone **2a** (1.2 equiv.), 4-DPAIPN (0.5 mol%). (E) Transient absorption spectra of PC (blue line) and PC + **1a** (0.1 M, red line) in aerated EtOAc solutions acquired 200 ns following pulsed excitation (355 nm, 5 ns pulse width, 20 mJ per pulse). Spectra were corrected for PC fluorescence. Inset shows transient absorption decay at 484 nm (20 mJ per pulse). Black lines are best fit according to a mono-exponential decay function, see text for details. (F) Binding isotherm between **1a** (5 mM) and PC in CD_2Cl_2 derived from the chemical shift of the OH proton in **1a**. Red line is best fit through the points with a binding constant of 18 M^{-1}.

such as DMSO and EtOAc, superoxide is known to be only weakly stabilized relative to its behavior in protic or aqueous media.[23] Consequently, the EPR signals corresponding to the DMPO–OOH adduct are typically weak and transient, often decaying within 1–15 min (see SI).[28] When the same experiment was performed in the presence of 2,2,6,6-tetramethylpiperidine (TEMP), the spectrum displayed the characteristic signal of TEMPO, confirming the concomitant generation of singlet oxygen (Fig. 4D). This observation is consistent with the results of the trapping experiments described above (Fig. 3B), collectively supporting the presence of both $O_2^{\bullet-}$ and $^1O_2$ in the reaction medium.

Based on these observations, a plausible reaction mechanism emerges as summarized in Fig. 5. Upon photoexcitation, the singlet excited state (S_1) of 4-DPAIPN (^{1}PC) is populated, which can undergo intersystem crossing (ISC) to generate the longer-lived triplet state (T_1, ^{3}PC).[18,19] 4-DPAIPN effectively possesses a high triplet quantum yield (Φ_T) owing to efficient ISC due to the small singlet–triplet energy gap (ΔE_{S-T}). The triplet state's long lifetime (τ_T = 84 μs) makes it well-suited to sensitize oxygen and generate reactive oxygen species (ROS).[19] As mentioned above, both singlet and triplet states are capable of interacting with ground-state molecular oxygen. Back-electron transfer or energy transfer from ^{3}PC can yield $^1O_2$ and explain its observation by trapping experiments. Moreover, with an excited-state oxidation potential of $E_{(PC^*/PC^{\bullet-})} = +1.10$ V (*vs.* SCE), 4-DPAIPN lacks the oxidative power to directly oxidize oximes ($E^{\circ}_{1/2} \sim +1.8 - 2.0$ V).[15,29] In contrast, it can effectively reduce molecular oxygen into superoxide, ($E_{(PC^*/PC^{\bullet+})} = -1.28$ V *vs.* $E_{(O_2/O_2^{\bullet-})} = -0.87$ V *vs.* SCE in CH_3CN). The preferential reaction of PC* with oxygen *versus* oxime is confirmed by fluorescence quenching experiments, which evidence efficient quenching by the former and no quenching for the latter (Fig. 4A and B).

Tortosa and co-workers recently reported the oxidative quenching of related 4-CzIPN by isonitriles, confirming the formation of 4-CzIPN$^{\bullet+}$ by comparing the transient absorption spectrum with that generated in the presence of a strong oxidant ($SbCl_5$).[30] Fig. 4E shows the transient absorption spectrum acquired using laser flash photolysis of aerated solutions of 4-DPAIPN in EtOAc. It possesses maxima at 484 nm and 580 nm, closely resembling that previously reported for 4-CzIPN$^{\bullet+}$. Upon addition of **1a**, the intensity of the transient absorption is diminished, suggesting that the PC$^{\bullet+}$ formed in the presence of oxygen reacts with the oxime. To probe the kinetics of the reaction between PC$^{\bullet+}$ and **1a**, the absorption at 484 nm was monitored. Interestingly, there is little difference in the decay kinetics of the transient, which are nearly identical within the experimental error (inset Fig. 4E). However, the initial intensity of the signal in the presence of **1a** is significantly reduced and represents *ca.* half of that observed in its absence. Such behavior can be indicative of a static quenching, a condition in which the quencher is bound or in close vicinity to the probe when excited by light. In such cases, the quenching process can be faster than the time resolution of the instrument (*ca.* 15 ns for this setup) and results in a reduced intensity of the signal at t = 0. In aprotic non-polar solvents such as EtOAc, H-bonding between the oxime's OH proton and the tertiary amines of the PC may contribute to establishing a favorable ground state interaction that can manifest as a downfield shift in the ^{1}H NMR spectrum.[31] Indeed, a 0.3 ppm shift and broadening of the OH proton in **1a** is observed upon addition of 4-DPAIPN (see ESI for details). Fitting of the binding isotherm at low concentrations, where the 1 : 1 adduct is favored results in a binding constant of 18 M^{-1} being determined in CD_2Cl_2 (Fig. 4F). This corresponds to a binding energy of $\Delta G = -7.3$ kJ mol^{-1}, which agrees with that expected for a single H-bond.

From these experiments, it emerges that the reaction sequence begins with the ground-state association of the PC with the oxime through H-bonding (*i.e.* ***i***) (Fig. 5). When this complex is excited in the visible, the **1**-PC*$\boldsymbol{ii}$ initially formed reacts with oxygen to produce **1**-PC$^{\bullet+}$ ***iii*** and superoxide. Electron transfer from the oxime to PC$^{\bullet+}$ within ***iii*** provides the iminoxyl radical ***iv***,[24,32,33] and restores PC in its ground state, ready to associate with **1** to give ***i***. The relatively low quantum yield ($\Phi = 9.5 \times 10^{-4}$, see SI) rules out a radical chain mechanism, and is consistent with light serving only to initiate the reaction rather than sustaining catalytic turnover. Although PC$^{\bullet+}$ does not possess sufficient oxidative potential to directly oxidize oximes, the H-bonding interaction in ***iii*** is proposed to facilitate electron transfer from the oxime to PC$^{\bullet+}$ by increasing

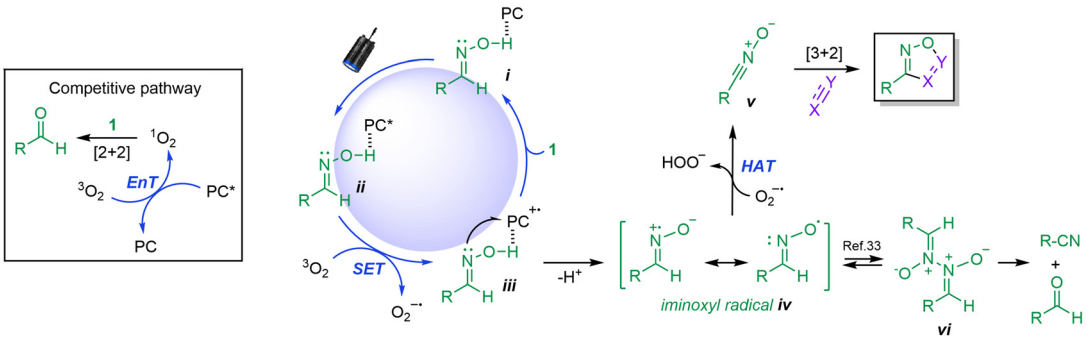

Fig. 5 Putative mechanism for the 4-DPAIPN-photocatalyzed oxidation of oximes **1** in the presence of ketones, nitriles and alkynes.

the electron density on the hydroxyl group. This effect is consistent with the reported strong dependence of H-bonding interactions on redox potentials.[34] The formation of ***iv*** is then supported by the detection of heterocycle **14** resulting from a 5-*endo*-trig cyclization onto the olefin of **13** (Fig. 3C).[24] Species ***iv*** are σ-radicals, having their unpaired electron in a π-type orbital located in the nodal plane of the C=N π-bond, and therefore cannot delocalize into the C=N π-system, which may also explain the absence of cyclopropane ring opening in **15** (Fig. 3C).[32,33] The ensuing iminoxyl radical ***iv*** then undergoes hydrogen atom abstraction by the superoxide radical generated in its vicinity to yield nitrile oxide ***v***,[35] which experiences [3 + 2] cycloaddition with ketones, nitriles, or alkynes to form the corresponding heterocycles **I–III**. In several experiments where heterocycles **I–III** were not formed, aldehydes were recovered as the major products. These may arise from a competing [2 + 2] cycloaddition involving singlet oxygen ($^1O_2$), as recently proposed.[14] An alternative pathway involving the reversible dimerization of radical ***iv*** into azine bis-*N*-oxide ***vi*** known to decompose into aldehydes and nitriles as observed above (*i.e.* **14b–c**, **16–17**) cannot be ruled out.[15a,29,32b,33]

Experimental

The oxime **1** (1.00 mmol, 1 eq.) and 4-DPAIPN (3% mole) were placed into a 20 mL resealable Schlenk tube equipped with a magnetic stirring bar and a Teflon septum, then ketone **2** or nitrile **4** or alkyne **6** (3.0 mmol, 3.0 eq.) were placed into the tube. EtOAc (0.1 M) was then added. An air balloon was then connected to the reactor septum *via* a needle. The reaction mixture was stirred vigorously for 5 minutes (sonicated if needed) then left under blue LED (456 nm) irradiation at 35 °C (±2 °C). A fan was installed near the reactor to maintain the temperature inside the tube around this temperature (SI). The reaction was monitored by TLC. Upon completion (~8 h), the reaction mixture was transferred to a round-bottom flask and the solvent evaporated under reduced pressure. The residue was purified by column chromatography on silica gel (petroleum ether/EtOAc 10 : 1), to afford the desired products **3**, **5** or **7** respectively.

Conclusions

In summary, we have developed a metal-free photocatalytic oxidation of oximes in the presence of ketones, nitriles, and alkynes, employing 4-DPAIPN as the photocatalyst under visible-light irradiation and an atmosphere of air. This protocol provides a green and efficient approach to three distinct families of heterocycles—1,2,4-oxadiazoles, isoxazoles, and 1,4,2-dioxazoles. In depth mechanistic investigations using EPR, fluorescence quenching experiments and transient absorption spectroscopy suggest that the reaction proceeds *via* the formation of an iminoxyl radical generated through oxidation of the oxime bound to the photocatalyst. The close spatial association between the oxime and the active catalytic species promotes the oxidation of the former. This phenomenon—which to our knowledge is unprecedented for this class of photocatalysts—is intriguing and points to opportunities for broader application. The iminoxyl radical then undergoes subsequent oxidation to generate a nitrile oxide intermediate eventually involved in a [3 + 2] cycloaddition with various dipolarophiles to afford the corresponding heterocyclic products. This operationally simple strategy exhibits broad substrate scope, tolerating both aromatic and aliphatic oximes, and generally furnishes the desired heterocycles in high yields, with reduced environmental impact, using benign oxygen as the terminal oxidant and low-toxicity EtOAc as a solvent, thereby circumventing classical stoichiometric strategies, producing significant amount of waste.

Author contributions

The manuscript was written through contributions of all authors. All authors have given approval to the final version of the manuscript.

Conflicts of interest

There are no conflicts to declare.

Data availability

All supporting data are provided within the article and its accompanying supplementary information (SI). Supplementary information: experimental details, synthetic procedures, structural characterization (^{1}H, ^{13}C, ^{19}F NMR, HRMS), spectroscopic data, and EPR and fluorescence experiments. See DOI: https://doi.org/10.1039/d5gc06840a.

CCDC 2489789 and 2489790 (**7i** and **3e**) contain the supplementary crystallographic data for this paper.[36a,b]

Acknowledgements

YM thanks the Consulat Général de France à Jérusalem for a PhD grant. We are grateful to the French government in the framework of the University of Bordeaux's IdEx "Investments for the Future" program/Grand Programme de Recherche entitled Post-Petroleum Materials (PPM) for a postdoctoral grant to AZ, as well as the ANR (GreeNCO, No. 24-CE07-4305-01) and the CNRS for financial support. We acknowledge the analytical facilities CESAMO for NMR, mass spectrometry and DRX studies.

References

1 (*a*) R. M. Bhat, V. Hegde, S. Budagumpi, V. Adimule and R. S. Keri, Benzimidazole–Oxadiazole Hybrids—Development in Medicinal Chemistry: An Overview, *Chem. Biol. Drug Des.*, 2024, **104**, e14609; (*b*) M. Camci and N. Karali, Bioisosterism: 1,2,4-Oxadiazole Rings, *ChemMedChem*, 2023, **18**, e202200638.

2 (*a*) J. Zhu, J. Mo, H. Lin, Y. Chen and H. Sun, The recent progress of isoxazole in medicinal chemistry, *Bioorg. Med. Chem.*, 2018, **26**, 3065–3075; (*b*) F. Hua and M. Szostak, Recent Developments in the Synthesis and Reactivity of Isoxazoles: Metal Catalysis and Beyond, *Adv. Synth. Catal.*, 2015, **357**, 2583–2614.

3 J. Plumet, The 1,3-Dipolar Cycloaddition Reactions of Nitrile Oxides in Water Media, *Curr. Org. Chem.*, 2021, **25**, 2683–2707.

4 P. Catalfomo and C. H. Eugster, Muscarine and Muscarine Isomers in Selected Inocybe Species, *Helv. Chim. Acta*, 1970, **53**, 848–851.

5 A. M. Jones and J. M. Helm, Emerging treatments in cystic fibrosis, *Drugs*, 2009, **69**, 1903–1910.

6 H. Ye, H. Wu, L. Chen, S. Ma, K. Zhou, G. Yan, J. Shen, D. Chen and S.-J. Su, Synthesis, Properties, Calculations and Applications of Small Molecular Host Materials Containing Oxadiazole Units with Different Nitrogen and Oxygen Atom Orientations for Solution-Processable Blue Phosphorescent OLEDs, *Electron. Mater. Lett.*, 2018, **14**, 89–100.

7 (*a*) H. Zhang, Y. Zou, X. Hao, Z. Dong and Z. Ye, Based on 1,2,4-Oxadiazole: Design and Synthesis of a Series of Insensitive Energetic Materials and Discovery of Another Route for the Synthesis of DNAF via Rearrangement, *J. Org. Chem.*, 2025, **90**, 2950–2957; (*b*) Y. Qu and S. P. Babailov, Azo-linked high-nitrogen energetic materials, *J. Mater. Chem. A*, 2018, **6**, 1915–1940.

8 (*a*) K. Hemming, Product Class 6: 1,2,4-Oxadiazoles, in *Science of Synthesis*, Thieme Verlag, 2004; (*b*) B. J. Wakefield, Product Class 9: Isoxazoles, in *Science of Synthesis*, 2004, Thieme Verlag; (*c*) T. M. V. D. Pinho e Melo, Recent Advances on the Synthesis and Reactivity of Isoxazoles, *Curr. Org. Chem.*, 2005, **9**, 925–958.

9 (*a*) J. A. Durden Jr. and D. L. Heywood, Reaction of "activated" esters with amidoximes. Convenient synthesis of 1,2,4-oxadiazoles, *J. Org. Chem.*, 1971, **36**, 1306–1307; (*b*) Z. Jakopin and M. S. Dolenc, Recent advances in the synthesis of 1,2,4- and 1,3,4-oxadiazoles, *Curr. Org. Chem.*, 2008, **12**, 850–898.

10 (*a*) *Synthetic Applications of 1,3-Dipolar Cycloaddition Chemistry toward Heterocycles and Natural Products*, ed. A. Padwa and W. H. Pearson, John Wiley & Sons, New York, 2002; (*b*) A. Quilico, G. Stagno d'Alcontres and P. Grünanger, A new reaction of ethylenic double bonds, *Nature*, 1950, **166**, 226–227; (*c*) M. Breugst and H.-U. Reissig, The Huisgen Reaction: Milestones of the 1,3-Dipolar Cycloaddition, *Angew. Chem., Int. Ed.*, 2020, **59**, 12293–12307; (*d*) V. Vullo, T. N. Danks and G. Wagner, Cycloaddition of Benzonitrile Oxide to Acetonitrile, Propyne and Propene – A Comparative Theoretical Study of the Reaction Mechanism and Regioselectivity, *Eur. J. Org. Chem.*, 2004, 2046–2052.

11 (*a*) V. Nair and T. D. Suja, Intramolecular 1,3-dipolar cycloaddition reactions in targeted syntheses, *Tetrahedron*, 2007, **63**, 12247–12275 and references therein; (*b*) B. A. Mendelsohn, S. Lee, S. Kim, F. Teyssier, V. S. Aulakh and M. A. Ciufolini, Oxidation of oximes to nitrile oxides with hypervalent iodine reagents, *Org. Lett.*, 2009, **11**, 1539–1542.

12 G. Zhao, L. Liang, C. H. E. Wen and R. Tong, In Situ Generation of Nitrile Oxides from NaCl–Oxone Oxidation of Various Aldoximes and Their 1,3-Dipolar Cycloaddition, *Org. Lett.*, 2019, **21**, 315–319 and references cited therein. .

13 (*a*) T. C. Pham, V.-N. Nguyen, Y. Choi, S. Lee and J. Yoon, Recent Strategies to Develop Innovative Photosensitizers for Enhanced Photodynamic Therapy, *Chem. Rev.*, 2021, **121**, 13454–13619; (*b*) M. C. DeRosa and R. J. Crutchley, Photosensitized singlet oxygen and its applications, *Coord. Chem. Rev.*, 2002, **233–234**, 351–371.

14 A. Savateev, N. V. Tarakina, V. Strauss, T. Hussain, K. ten Brummelhuis, J. M. Sánchez Vadillo, Y. Markushyna, S. Mazzanti, A. P. Tyutyunnik, R. Walczak, M. Oschatz, D. M. Guldi, A. Karton and M. Antonietti, Potassium Poly (Heptazine Imide): Transition Metal-Free Solid-State Triplet Sensitizer in Cascade Energy Transfer and [3 + 2]-cycloadditions, *Angew. Chem., Int. Ed.*, 2020, **59**, 15061–15068.

15 (*a*) S. Hofmann, J. Winter, T. Prenzel, M. de Jesús Gálvez-Vázquez and S. R. Waldvogel, Electrochemical Synthesis of Isoxazoles and Isoxazolines via Anodic Oxidation of Oximes, *ChemElectroChem*, 2023, **10**, e202300434; (*b*) S. D. L. Holman, A. G. Wills, N. J. Fazakerley, D. L. Poole, D. M. Coe, L. A. Berlouis and M. Reid, Electrochemical Synthesis of Isoxazolines: Method and Mechanism, *Chem. – Eur. J.*, 2022, **28**, e202103728; (*c*) A. A. Al-Romema, H. Xia, K. J. J. Mayrhofer, S. B. Tsogoeva and P. Nikolaienko, *In situ* Electrolyte for Electrosynthesis: Scalable Anodically Enabled One-Pot Sequence from Aldehyde to Isoxazol(in)es, *Chem. – Eur. J.*, 2024, **30**, e202402696.

16 (*a*) A. A. Ghogare and A. Greer, Using Singlet Oxygen to Synthesize Natural Products and Drugs, *Chem. Rev.*, 2016, **116**, 9994–10034; (*b*) A. G. Griesbeck and M. Cho, 9-Mesityl-10-methylacridinium: An Efficient Type II and Electron-Transfer Photooxygenation Catalyst, *Org. Lett.*, 2007, **9**, 611–613; (*c*) R. Costa e Silva, L. Olivera da Silva, A. de Andrade Bartolomeu, T. J. Brocksom and K. T. de Oliveira, Recent applications of porphyrins as photocatalysts in organic synthesis: batch and continuous flow approaches, *Beilstein J. Org. Chem.*, 2020, **16**, 917–955; (*d*) C. Grundke, R. C. Silva, W. R. Kitzmann, K. Heinze, K. T. de Oliveira and T. Opatz, Photochemical α-Aminonitrile Synthesis Using Zn-Phthalocyanines as Near-Infrared Photocatalysts, *J. Org. Chem.*, 2022, **87**, 5630–

5642; (*e*) H. Görner, Z. Miskolczy, M. Megyesi and L. Biczók, Photooxidation of Alkaloids: Considerable Quantum Yield Enhancement by Rose Bengal-sensitized Singlet Molecular Oxygen Generation, *Photochem. Photobiol.*, 2011, **87**, 1315–1320.

17 Y. Wu, J. Kang, H. Zhu, M. Bi, J. Li, Q. Meng, X. Lyu and Z. Wu, Photocatalytic Strategy to Realize N-Debenzylation via Aerobic Oxidation Catalyzed by 4CzIPN, *ACS Sustainable Chem. Eng.*, 2024, **12**, 6640–6647.

18 (*a*) A. Brydena and E. Zysman-Colman, Organic thermally activated delayed fluorescence (TADF) compounds used in photocatalysis, *Chem. Soc. Rev.*, 2021, **50**, 7587–7680; (*b*) A. Tlili and S. Lakhdar, Acridinium Salts and Cyanoarenes as Powerful Photocatalysts: Opportunities in Organic Synthesis, *Angew. Chem., Int. Ed.*, 2021, **60**, 19526–19549.

19 (*a*) J. Luo and J. Zhang, Donor–Acceptor Fluorophores for Visible-Light-Promoted Organic Synthesis: Photoredox/Ni Dual Catalytic C(sp3)–C(sp2) Cross-Coupling, *ACS Catal.*, 2016, **6**, 873–877; (*b*) P. P. Singh and V. Srivastava, Recent advances in using 4DPAIPN in photocatalytic transformations, *Org. Biomol. Chem.*, 2021, **19**, 313–321.

20 S. Morrocchi, A. Ricca and L. Velo, The catalytic action of BF_3 in the cycloaddition of benzonitrile oxide with nitriles and carbonyl compounds, *Tetrahedron Lett.*, 1967, **8**, 331–334.

21 (*a*) B. C. Sanders, F. Friscourt, P. A. Ledin, N. E. Mbua, S. Arumugam, J. Guo, T. J. Boltje, V. V. Popik and G.-J. Boons, Metal-Free Sequential [3 + 2]-Dipolar Cycloadditions using Cyclooctynes and 1,3-Dipoles of Different Reactivity, *J. Am. Chem. Soc.*, 2011, **133**, 949–957; (*b*) A. M. Jawalekar, E. Reubsaet, F. P. J. T. Rutjes and F. L. van Delft, Synthesis of isoxazoles by hypervalent iodine-induced cycloaddition of nitrile oxides to alkynes, *Chem. Commun.*, 2011, **47**, 3198–3200.

22 J. Park, H. Tang and P. Zhang, Differentiation of superoxide radical anion and singlet oxygen and their concurrent quantifications by nuclear magnetic resonance, *Anal. Chem.*, 2023, **95**, 5293–5299.

23 M. Hayyan, M. A. Hashim and I. M. Al Nashef, Superoxide Ion: Generation and Chemical Implications, *Chem. Rev.*, 2016, **116**, 3029–3085.

24 H. Llantén, S. Barata-Vallejo, A. Postigo and P. A. Colinas, Synthesis of C-glycosylmethyl isoxazoles via aerobic oxidation of ketoximes catalyzed by TEMPO, *Tetrahedron Lett.*, 2017, **58**, 1507–1511.

25 Y. Tamaki, K. Kamogawa, R. Inoue, P. Ceroni and O. Ishitani, Importance of Selective Quenching of the Triplet Excited State of Thermally Activated Delayed Fluorescence (TADF) Photosensitizers in Redox-Photosensitized Reactions: Case Studies on Photocatalytic CO_2 Reduction, *J. Am. Chem. Soc.*, 2025, **147**, 33010–33022.

26 (*a*) A. Schumpe and P. Luehring, Oxygen Diffusivities in Organic Liquids at 293.2 K, *J. Chem. Eng. Data*, 1990, **35**, 24–25; (*b*) R. Battino, T. R. Rettich and T. Tominaga, The Solubility of Oxygen and Ozone in Liquids, *J. Phys. Chem. Ref. Data*, 1983, **12**, 163–178.

27 (*a*) E. Finkelstein, G. M. Rosen and E. J. Rauckman, Spin Trapping. Kinetics of the Reaction of Superoxide and Hydroxyl Radicals with Nitrones, *J. Am. Chem. Soc.*, 1980, **102**, 4994–4999; (*b*) G. M. Rosen and B. A. Freeman, Detection of superoxide generated by endothelial cells, *Proc. Natl. Acad. Sci. U. S. A.*, 1984, **81**, 7269–7273.

28 (*a*) D. T. Sawyer and J. S. Valentine, How Super Is Superoxide?, *Acc. Chem. Res.*, 1981, **14**, 393–400; (*b*) C. P. Andrieux, P. Hapiot and J. M. Saveant, Mechanism of superoxide ion disproportionation in aprotic solvents, *J. Am. Chem. Soc.*, 1987, **109**, 3768–3775.

29 H. P. De Lijser, S. Hsu, B. V. Marque, A. Park, N. Sanguantrakun and J. R. Sawyer, Effect of structure in benzaldehyde oximes on the formation of aldehydes and nitriles under photoinduced electron-transfer conditions, *J. Org. Chem.*, 2006, **71**, 7785–7792.

30 I. Quirós, M. Martín, M. Gomez-Mendoza, M. J. Cabrera-Afonso, M. Liras, I. Fernández, L. Nóvoa and M. Tortosa, Isonitriles as Alkyl Radical Precursors in Visible Light Mediated Hydro- and Deuterodeamination Reactions, *Angew. Chem., Int. Ed.*, 2024, **63**, e202317683.

31 (*a*) V. T. Nguyen, V. D. Nguyen, G. C. Haug, H. T. Dang, S. Jin, Z. Li, C. Flores-Hansen, B. S. Benavides, H. D. Arman and O. V. Larionov, Alkene Synthesis by Photocatalytic Chemoenzymatically Compatible Dehydrodecarboxylation of Carboxylic Acids and Biomass, *ACS Catal.*, 2019, **9**, 9485–9498; (*b*) T. Inoue, D. Tomiya, M. Fuki, Y. Kobori, M. Higashi, K. Uesaka, A. Yamakata, S. A. Kawashima, K. Yamatsugu, H. Mitsunuma and M. Kanai, Azaanthraquinone PCET Catalysis Enables Chemoselective Decarboxylative Functionalization of Diverse Carboxylic Acids, *J. Am. Chem. Soc.*, 2025, **147**, 40272–40281.

32 (*a*) D. A. Pratt, J. A. Blake, P. Mulder, J. C. Walton, H.-G. Korth and K. U. Ingold, O-H Bond Dissociation Enthalpies in Oximes: Order Restored, *J. Am. Chem. Soc.*, 2004, **126**, 10667–10675; (*b*) I. B. Krylov, S. A. Paveliev, A. S. Budnikov and A. O. Terent'ev, Oxime radicals: generation, properties and application in organic synthesis, *Beilstein J. Org. Chem.*, 2020, **16**, 1234–1276.

33 J. L. Brokenshire, J. R. Roberts and K. U. Ingold, Kinetic applications of electron paramagnetic resonance spectroscopy. VII. Self-reactions of iminoxy radicals, *J. Am. Chem. Soc.*, 1972, **94**, 7040–7049.

34 (*a*) R. Ashizawaa and T. Noguchi, Effects of hydrogen bonding interactions on the redox potential and molecular vibrations of plastoquinone as studied using density functional theory calculations, *Phys. Chem. Chem. Phys.*, 2014, **16**, 11864–11876; (*b*) R. Liu, H. Wang and K. Xu, Non-covalent interactions for redox potential modulation in organic electrosynthesis, *Chem. Commun.*, 2025, **61**, 18608–18620.

35 (*a*) E. J. Nanni, M. D. Stallings and D. T. Sawyer, Does Superoxide Ion Oxidize Catechol, α-Tocopherol, and Ascorbic Acid by Direct Electron Transfer?, *J. Am. Chem.*

Soc., 1980, **102**, 4481–4485; (*b*) E. J. Nanni and D. T. Sawyer, Superoxide-ion oxidation of hydrophenazines, reduced flavins, hydroxylamine, and related substrates via hydrogen-atom transfer, *J. Am. Chem. Soc.*, 1980, **102**, 7591–7593.

36 (*a*) CCDC 2489789: Experimental Crystal Structure Determination, 2026, DOI: 10.5517/ccdc.csd.cc2pktsw; (*b*) CCDC 2489790: Experimental Crystal Structure Determination, 2026, DOI: 10.5517/ccdc.csd.cc2pkttx.